Chalcogenide Letters Vol. 10, No. 5, May 2013, p. 159 - 165

INFLUENCE OF UTLTRASOUNDS ON STRUCTURAL AND MORPHOLOGICAL PROPERTIES OF PbS DEPOSITED ON GLASS SUBSTRATE

V. POPESCU[a,b], D. RĂDUCANU[c], A. DINESCU[a], M. DĂNILĂ[a]
G. L. POPESCU [b,*]
[a]*National Institute for Research and Development in Microtechnologies, IMT, 077190 Bucharest, Romania.*
[b] *Technical University of Cluj-Napoca, 103-105 Muncii Avenue, 400641 Cluj-Napoca, Romania*
[c]*Politehnica University, Splaiul Independenţei 313, 060042, Bucharest, Romania*

Chemical bath deposition (CBD) and ultrasonic chemical bath deposition (US-CBD) on glass substrates of PbS crystals from lead nitrate, thiourea alkaline aqueous solutions have been studied. The influence of the ultrasonic vibration on the PbS crystals deposition by CBD through observing the changes in structure and morphology was studied. Structural properties were investigated by X ray – diffraction and the average grain size has been calculated applying different methods. Ultrasounds lead to an increase of crystallites size and strain. SEM micrographs showed that the PbS obtained from static baths are formed from near spherical grains with average size of 183 nm while in the case of ultrasonic baths cubical particles of 257 nm were formed.

(Received April 1, 2013; accepted April 30, 2013)

Keywords: lead sulfide, chemical bath deposition, X-ray diffraction, SEM, ultrasounds.

1. Introduction

PbS is an important binary IV-VI semiconductor material with narrow band gap (Eg) (0.41 eV at 300 K) having the Eg very sensitive to grain size, which makes it a good candidate for nanostructured devices.

Because the main property of PbS semiconductor is the band gap, new methods for controlling and influencing the grain size that influences the band gap is of high interest. Sonochemical methods are used for the increasing of reaction rate and for obtaining of materials with special properties. The influence of ultrasonic (US) irradiation on the formation of films of crystals by chemical bath deposition (CBD) was rarely approached and it worth to be investigated for the optimization of the deposition processes, or for the reducing of the reaction time.

As far as we know, there are no data in literature related to PbS crystals or films obtaining by sonochemical methods on glass substrates; although, sonochemical methods were studied to obtain PbS nanoparticles [1-9], nanobelts [7], or microtubes [10]. Depending on the surfactant concentration, sonication time and lead salt, Wang et al. obtained cubes, spheres, rods and tubes [8]. For short sonication time spherical or cubical crystals are formed, while for longer sonication time nanorods [9], nano/microtubes [9,10] or nanobelts [7] can be obtained.

The solvents use for sonochemical synthesis influence the formation of PbS particles [3].

The paper presents the influence of ultrasounds on structural and morphological properties of PbS crystals deposited on glass substrate. Previous studies presented the influence of ultrasounds on electrical, photoelectrical [11] and optical [12] properties of PbS films. In this study we reduced the concentration of reagents and introduced hydroxylamine hydrochloride in the bath.

* Corresponding author: georgepopescu60@gmail.com

2. Experimental details

PbS was deposited on microscopic glass slides, from baths containing 0.014 M/L lead nitrate, 0.029 M/L thiourea, 0.3 M/L NaOH and 0.002 m/L hydroxylamine hydrochloride, at 35± 2°C for 40 minutes. The deposition took places in two beakers; the first was placed in a thermostatic bath (Raypa BOE-2) for static (S) deposition and the other one in an ultrasonic bath (Elma Sonic S 30 H) for sonochemical (US) deposition at the frequency of 37 kHz. For avoiding the increasing of the temperature under US conditions, the bath was cooled using a copper spiral in which cold water was circulated using a Low temperature Bath DC 100 G.

At temperatures of 25-30°C no PbS was formed on the glass substrate in the presence of US.

X-ray diffraction measurements were performed on a 9 kW triple axis rotating anode Rigaku SmartLab thin film diffraction system (Rigaku, Japan), using standard thin films X-ray measurement technique with $CuK\alpha_{1,2}$ radiation.

Field emission scanning electron microscope – Raith e_Line with in-lens electron detection capabilities was used for morphological characterization. Since the substrate is an insulator, in order to avoid the electrostatic charging we used low accelerating voltages and a low beam current.

3. Results and discussions

3.1 Structural properties

PbS depositions were analyzed by XRD methods with the aim to establish the influence of ultrasounds on the deposited PbS microstructure and to calculate the crystallite's sizes. X-ray diffraction patterns are presented in Figure 1. The strong and sharp diffraction peaks indicated that the as-prepared PbS depositions are well-crystalline. All diffraction peaks can be indexed to face-centered-cubic rocksalt structured PbS crystal (JCPDS 5-592, a=5.936 Å).

US lead to the increase of the intensity of diffraction lines and the line become narrower. Because the determination conditions were the same for both samples we concluded that the crystallinity and the crystal sizes of the US-PbS sample increased, which suggests a higher growth rate under ultrasonic irradiation.

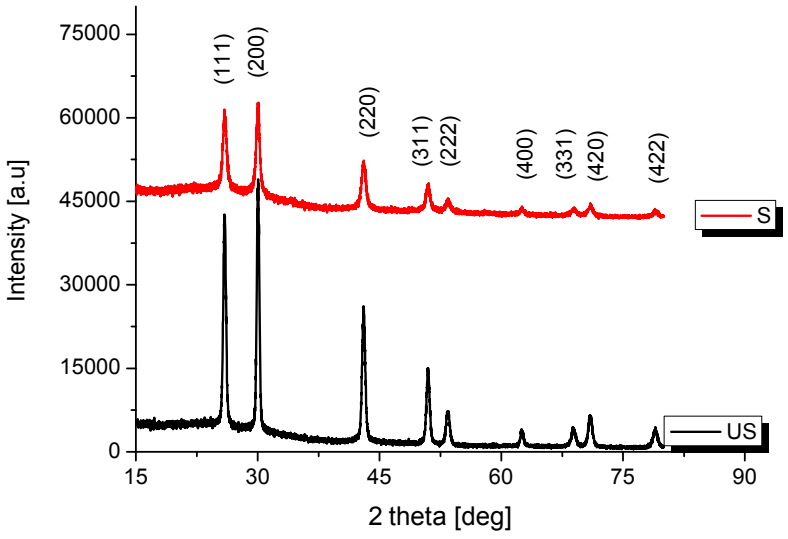

Fig. 1. X-ray diffraction pattern of PbS crystals obtained under static (sample S) and ultrasonic (sample US) conditions on glass substrate.

One can also observe that the intensity of the (200) reflection is higher than that of the (111) reflection [13]. According to Masoud Mozafari [14], the possibility to obtain the shape of a face center cubic (FCC) crystal is mainly determined by the ratio of the growth rate in the ⟨100⟩ direction and ⟨111⟩ directions. When the ratio is relatively high, PbS cubes bounded by the six {100} crystalline planes will be formed, otherwise, rods tend to form [14,15]. No obvious characteristic diffraction peaks of any other impurities such as PbO, PbO_2, $PbSO_3$, $PbSO_4$ or other precursor compounds can be detected [14].

The interplanar distances (d_{hkl}) (Table 1) for each diffraction angle have been calculated using Bragg's low:

$$d_{hkl}=n\cdot\lambda/2\cdot\sin\theta \quad (1)$$

where λ is X-ray wavelength (λ = 1.54059292 [Å]) and θ Bragg diffraction angle.

There is a good correlation between the d_{hkl} of the PbS crystals with the values from JCPDS card indicating the formation of a pure well crystallized PbS.

Table 1. Interplanar distances (d_{hkl}), crystallite size (D) (estimated using Scherrer relation) and lattice constant (a)

d_{hkl} [Å]			D [Å]		a [Å]		(hkl)
JCPDS 5 0592	S	US	S	US	S	US	
3.429	3.432	3.433	144	199	5.9438	5.9464	(111)
2.969	2.973	2.971	160	224	5.9459	5.9426	(200)
2.099	2.099	2.099	137	190	5.9361	5.9372	(220)
1.790	1.790	1.790	148	189	5.9360	5.9358	(311)
1.714	1.713	1.714	136	168	5.9339	5.9360	(222)
1.484	1.484	1.484	164	206	5.9358	5.9348	(400)
1.362	1.361	1.362	140	168	5.9326	5.9353	(331)
1.327	1.327	1.327	146	170	5.9337	5.9344	(420)
1.212	1.211	1.211	144	157	5.9333	5.9339	(422)

There is a good correlation between the d_{hkl} of the PbS crystals with the values from JCPDS card indicating the formation of a pure well crystallized PbS.

The crystallite's size (table 1) of crystals has been estimated using Scherrer's formula:

$$D=0.9\cdot\lambda/\beta\cdot\cos\theta \quad (2)$$

Lattice constant (a) (Table 1) has been calculated for PbS particles for each diffraction line with the relation [16]:

$$a^2=d^2(h^2+k^2+l^2)\ [Å] \quad (3)$$

where h, k and l are the Miller indices.

The corrected values of lattice constants were estimated by extrapolating to θ = 90° of the Nelson–Riley [17] plots:

$$f(\theta) = 1/2(\cos^2\theta/\sin\theta + \cos^2\theta/\theta) \quad (4)$$

The values a = 5.929 Å (samples S) and 5.930, (sample US) obtained from Nelson Riley plots (Fig. 2), were close to the value from the JCPDS (a_o = 5.936 Å). The small difference between the lattice constant for PbS crystals comparing to the crystals of bulk can be caused by some non-uniform strain of the sample [18].

Because the lattice constant is slightly different comparing to the value from JCPDS, a better estimation for the size of the crystallite can be made using the Williamson-Hall (WH) method [19-21], based on the relation:

$$\beta \cdot \cos\theta = k \cdot \lambda / D + 4 \cdot \varepsilon \cdot \sin\theta \quad (5)$$

where ε is the strain and k a constant.

The strain and the crystallite size can be determined from the slope (4·ε) and from the intercept (k·λ/D) respectively of the plot of $\beta \cdot \cos\theta = f(\sin\theta)$. Figure 3.a presents the WH plots for PbS samples. The correlation factors (R^2) from WH plots are very small (0.08 for sample S and 0.21 for sample US), leading to the conclusion that other methods would work better for the estimation of the crystallite's size and strain. Following this conclusion, the crystallite size (table 2) and strain (Fig. 3 b) have been further determined using a Modified form of Williamson Hall (MWH) relation, from the plot of $\beta/tang\theta = f(1/\sin\theta)$ using the equation 6:

$$\beta/\text{tang}\theta = (k \cdot \lambda/D) \cdot 1/\sin\theta + 4\varepsilon \quad (6)$$

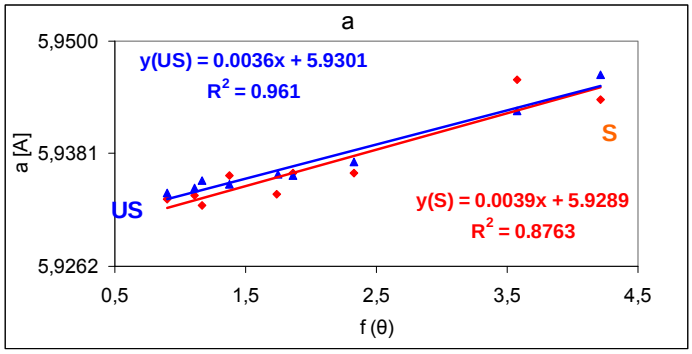

Fig. 2. The determination of lattice constant for PbS samples by extrapolation of Nelson–Riley plots

The size of the crystallite was determined from the slope (k·λ/D) and the strain (4·ε) from the intercept of the plot $\beta/tang\theta = f(1/\sin\theta)$ (Table 2).

A very good linearization can be obtained using Halder Wagner (HW) [22,23] plots:

$$(\beta^2/(\tan\theta)^2 = (k \cdot \lambda/D)(\beta/\tan\theta \cdot \sin\theta) + 16\,\varepsilon^2) \quad (7)$$

The size (D) was calculated from the slope $(k \cdot \lambda/D)$, while the strain was estimated from the intercept $(16\,\varepsilon^2)$ of the HW plots (Fig. 3 c).

The linearization is better when the MWH relation has been used allowing the calculation of D and ε with smaller errors.

The values obtained applying all the presented methods are close, and the differences can be considered as accepted errors for crystallite's size determination (Table 2). The average crystallite's size obtained applying the methods presented above have been taken into consideration for further discussions.

Table 2. The size and the strain of PbS crystallite

Sample	D_{HW} [nm]*	$Strain_{HW}$ [%]*	D_{WH} [nm]**	$Strain_{WH}$ [%]**	D_{MWH} [nm]***	$Strain_{MWH}$ [%]***
S	14.7	0.02	14.6	0.00	14.9	0.00
US	21.3	0.15	25.2	0.11	24.3	0.10
JCPDS 50 592	$*\beta^2/(\tan\theta)^2 = (k \cdot \lambda/D)(\beta/\tan\theta \cdot \sin\theta) + 16\,\varepsilon^2$; ** $\beta \cdot \cos\theta = k \cdot \lambda/D + 4 \cdot \varepsilon \cdot \sin\theta$; *** $\beta/tang\theta = (k \cdot \lambda/D) \cdot 1/\sin\theta + 4 \cdot \varepsilon$					

The US lead to the increasing of the average size of crystallite from 14.7 nm (S) to 23.6 nm (US) revealing an increase of reaction rate that can be explained by acoustic cavitation determined by ultrasounds. According to Jingjing Guo et al, acoustic cavitation imply the rapid formation, growth, and the collapse of bubbles in liquid. The extremely high local temperature (>5000 K), pressure (>20 MPa) and very high cooling rates (>1010 Ks^{-1}) confer sonicated solutions unique properties [24].

The increasing of the reaction rate for the obtaining of PbS crystals on glass slides with higher crystallite has been obtained by Obaid [25] under microwave exposure.

The strain increased from 0.01 (%) to 0.12 (%) in the case of the samples obtained under ultrasonic agitation (Table 2).

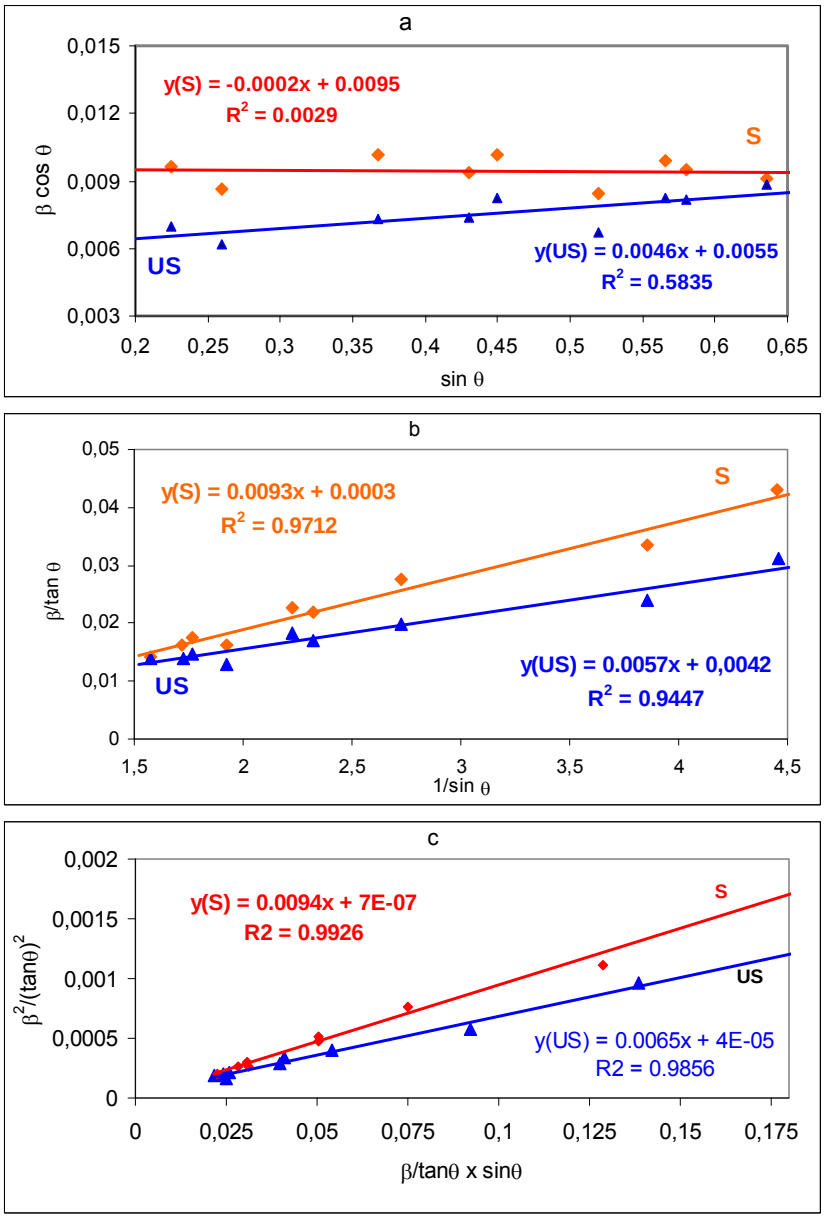

Fig. 3. Williamson Hall (a), modified Williams Hall (b) and Halder Wagner (c) plots for samples S and US

2.2. Morphological properties

Figure 4 presents SEM micrographs of the samples S and US, respectively. One can see that in the absence of ultrasounds the grains sizes are very uniform and cubooctahedron shaped. Particles with similar shapes were observed in the films obtained by Kumar et al [26].

The PbS - US crystals have also uniform sizes and distribution but exhibit cubic shapes. The grains increase comparing to the ones obtained in static bath from about 183 nm to 257 nm (fig. 4). Our results are quite different comparing to the results obtained by Rongguo Xie et al who presented a sonochemical method for obtaining other PbS entities: nanoparticles on silica spheres and PbS hollow structures by a sonochemical methods [27]. High intensity ultrasounds (40 kHz, 200 W) assured the formation of a nano-sized compact PbS layer on the surface of silica spheres, while in the absence of ultrasounds the PbS particles obtained by Rongguo Xie were much larger [27].

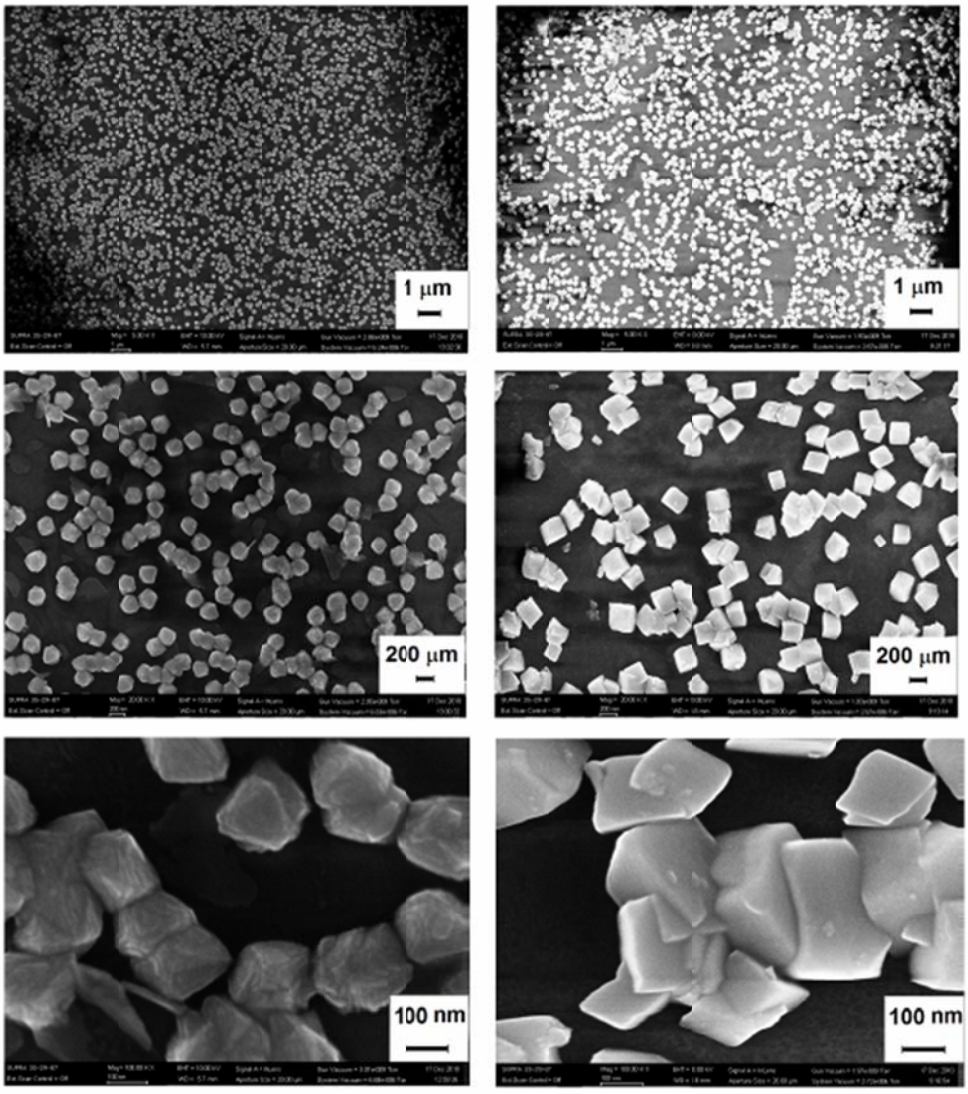

a b

Fig. 4. SEM images of PbS particles deposited on glass substrates under static (sample S column a) and ultrasonic (sample US column b) conditions.

We obtained similar results with Baojun Huang et al. [28] who showed that ultrasounds determined an important increase of the size of the particles that forms films of metal iodide (CuI, AgI and PbI_2), proving that US have a strong influence on the reaction rate. They concluded that ultrasounds drastically reduce the reaction time generally needed in other chemical methods [28].

3. Conclusions

We studied the influence of ultrasounds on structural and morphological properties of PbS crystals. Ultrasounds lead to the increase of crystallite's size from around 14.7 to around 21.3 nm; the increase of the strain from 0.01 % to 0.11 %; the increase of $I_{(111)}/I_{(200}$ ratio from 0.90 to 0.93 (standard value 0.85); the formation of cubical crystals of around 257 nm, instead of almost spherical ones of around 183 nm, indicating a different tropism of the crystals growth.

Acknowledgment

This paper was supported by the project "Dezvoltarea Resurselor Umane prin Cercetare Postdoctorala in Domeniul Micro si Nanotehnologiilor", Contract POSDRU/89/1.5/S/63700, project co-funded from European Social Fund through Sectorial Operational Program Human Resources 2007-2013.

References

[1] R. Xie, D. Li, D. Yang, M. Jiang, M., J. Mater. Sci. **42**, 1376 (2007).
[2] H. Wang, J. Zhang, J. - Zhu, J. Cryst. Growth. **246**, 161 (2002).
[3] Y. Zhao, X. Liao, J. Hong, J. & Zhu, Mater. Chem. Phys. **87**, 149 (2004).
[4] J. Zhu, S. Liu, O. Palchik, Y., Koltypin, A. Gedanken, J. Solid State Chem. **153**, 342 (2000).
[5] S. F. Wang, F. Gu, M. K. Lu, Langmuir **22**, 398 (2006).
[6] S. M., Zhou, Y. S. Feng, L. D. Zhang, J. Mater. Res. **18**, 1188 (2003).
[7] S. Zhou, X. Zhang, X. Meng, X., Fan, S. Lee, S. Wu, J. Solid State Chem. **178**, 399 (2005).
[8] S. Fen Wang, F. Gu, M. K. Lu, G. Jun Zhou, A. Yu Zhang, J. Cryst. Growth **289**, 621 (2006).
[9] Z. Xiu, S. Liu, J. Yu, F. Xu, W. Yu, G. Feng. J. Alloy. Compd. **457**, L9 (2008).
[10] W. Wang, Q. Li, M. Li, H. Lin, L. Hong, J. Cryst. Growth **299**, 17 (2007).
[12] V. Popescu, N. Jumate, G. L. Popescu, M. Moldovan, C. Prejmerean, Chalcogenide Lett. **7**(2), 95 (2010).
[11] V. Popescu, G. L. Popescu, M. Moldovan, C. Prejmerean**,** Chalcogenide Lett. 6, 503 (2009).
[13] S. Seghaier, N. Kamoun, R. Brini, A.B. Amara, Mater. Chem. Phys. **97**, 71 (2006).
[14] M. Mozafari, F. Moztarzadeh, J. Colloid. Interface Sci. **351**, 442 (2010).
[15] S.M. Lee, S.N. Cho, J. Cheon, Adv. Mater. **15**, 441 (2003).
[16] P. Thirumoorthy, P.K. Murali, J. Mater. Sci. Mater. El. **22**, 72 (2011).
[17] J.B. Nelson, D.P. Riley, Proc. Phys. Soc., London, **57**, 160, (1945).
[18] N. Choudhury and B. K. Sarma, Thin Solid Films, **31**, 2132 (2011).
[19] G. K. Williamson and W. H. Hall, Acta Metall. **1**, 22 (1953).
[20] D. Sahu, B.S. Acharya, A.K. Panda, Ultrason. Sonochem. **18**, 601 (2011).
[21] A.S. Obaid, M.A. Mahdi, Asmiet Ramizy, Z. Hassan, Adv. Mater. Res. **364**, 60 (2012).
[22] N. C. Halder, C. N. J. Wagner. Acta Crystallogr. **20**, 312 (1996).
[23] J. Xu, W. Menestklou, E. Ivers-Tiffée, J. Electroceram. **13**, 229 (2004).
[24] J. Guo, Z. Chen, Y. Li, Z. Yu, Q. Liu, J. Li, C. Feng, D. Zhang, Ultrason. Sonochem. **18**, 1082 (2011).
[25] A.S. Obaid, M.A. Mahdi, Z. Hassan, M. Bououdina, Mat. Sci. Semicon. Proc. **15**, 564 (2012).
[26] D. Kumar, G. Agarwal, B. Tripathi, D. Vyas, V. Kulshrestha, J. Alloys Compd. **484**, 463 (2009).
[27] R. Xie, D. Li, D. Yang, M. Jiang, M., J. Mater. Sci. **42**, 1376 (2007).
[28] B. Huang, Z. Zheng, F. Yang, Y. Zhang, D. Pu, H. Zhao, D. Li, Solid State Ionics, **179**, 2006 (2008).